Electronic Supplementary Material (ESI) for Physical Chemistry Chemical Physics.

Supporting information for: Nonlinear Optical Responses Of Self-Assembled Monolayers Functionalized With Indolino-Oxazolidine Photoswitches

Claire Tonnelé,[*,†] Kornelia Pielak,[‡,¶] Jean Deviers,[‡] Luca Muccioli,[§] Benoit Champagne,[*,¶] and Frédéric Castet[*,‡]

†*Institut des Sciences Moléculaires (ISM, UMR CNRS 5255), University of Bordeaux, 351 Cours de la Libération, 33405 Talence, France*

‡*Institut des Sciences Moléculaires (ISM, UMR CNRS 5255), University of Bordeaux, 351 Cours de la Libération, 33405 Talence, France*

¶*Unité de Chimie Physique Théorique et Structurale, Chemistry Department, Namur Institute of Structured Matter, University of Namur, Belgium*

§*Department of Industrial Chemistry "Toso Montanari", University of Bologna, Viale Risorgimento 4, 40136 Bologna, Italy*

E-mail: claire.tonnele@u-bordeaux.fr; benoit.champagne@unamur.be; frederic.castet@u-bordeaux.fr

Force field parameterization

Torsional potentials around the $\theta_1 - \theta_{10}$ dihedrals (Figure SI-1) were derived from DFT calculations performed at the M06/6-311G(d) level. The DFT and re-parameterized molecular mechanics torsional potentials are displayed in Figure SI-2.

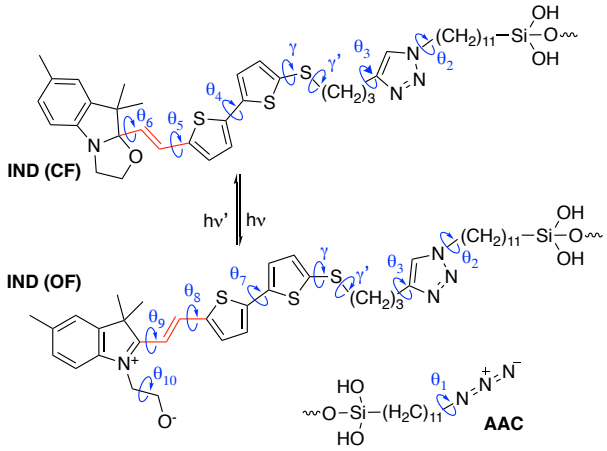

Figure SI-1: Scheme of the photochromic switchable closed form (CF) and open form (OF) of the indolino-oxazolidine (IND) derivative, and azido-undecylsilane chain (AAC). Force field parameters have been re-calculated for torsions θ_1 to θ_{10}. The dihedrals are defined as follows: θ_1 =NNCC, θ_2 =CCNC, θ_3 =NCCC, θ_4 =SCCS, θ_5 =SCCC, θ_6 =CCCN, θ_7 =SCCS, θ_8 =SCCC, θ_9 =CCCN, θ_{10} =NCCO, γ =CSCC, γ' =CSCC.

Preparation of the SiO_2 surface

Simulations were carried out using Clay force field[S1] to describe amorphous silica. A bulk sample was prepared following a procedure similar to the one reported by Della Valle *et al.*[S2] and described hereafter. A box of dimensions $52.044 \times 51.119 \times 30.000$ Å^3 was filled with 1745 Si atoms and 3490 O atoms randomly distributed (using Packmol[S3]) to achieve the experimental density[S4] of vitreous silica at room temperature (2.2 g·cm^{-3}). An energy minimization was performed to avoid possible steric clashes or irregularities in the input structure, applying 3D periodic boundary conditions. The sample was then heated up to 4000 K (i) for the first 100 ps, a 0.2 fs timestep was used and velocities rescaled every step,

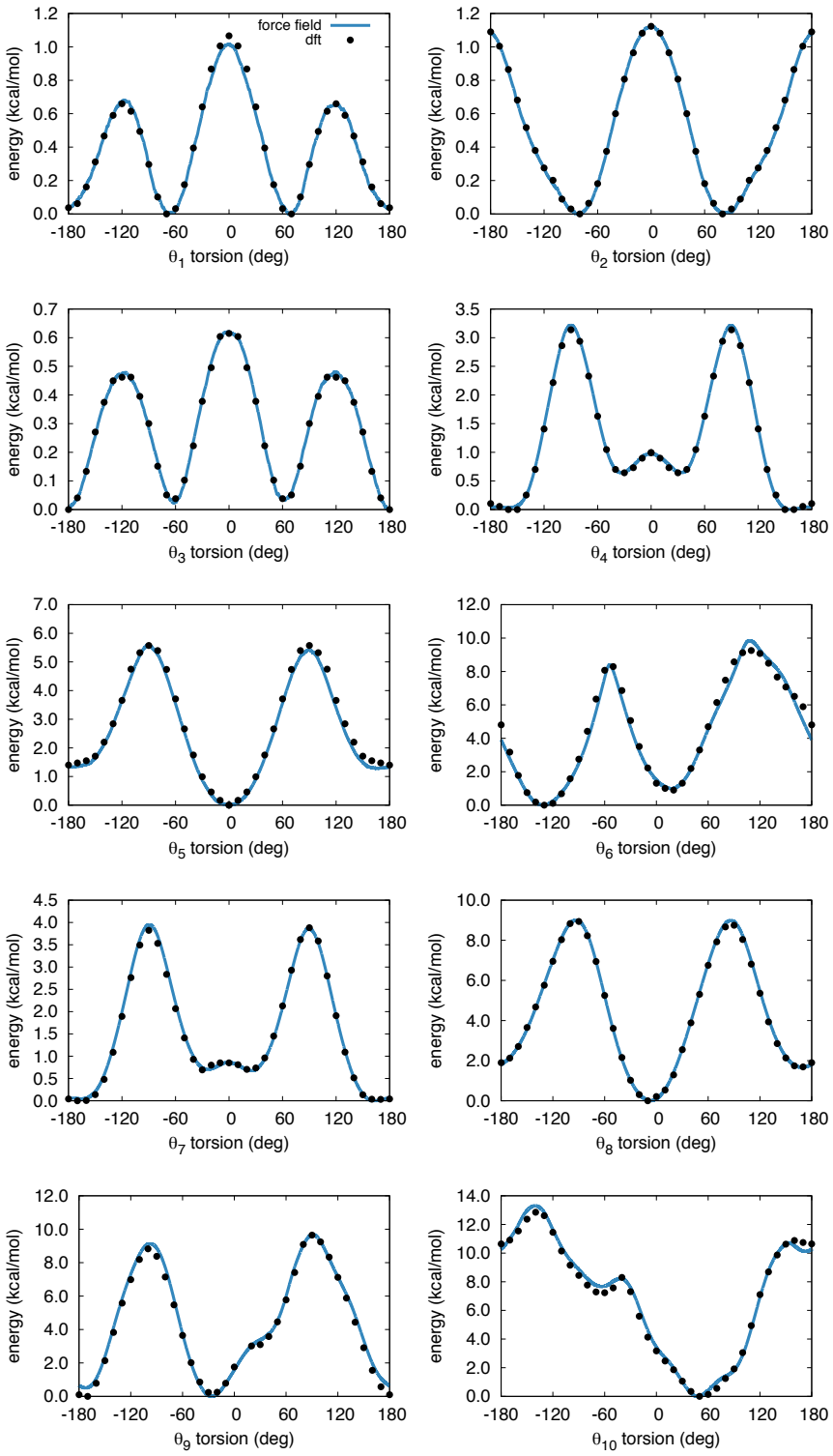

Figure SI-2: DFT and re-parameterized molecular mechanics torsional potentials around dihedrals $\theta_1 - \theta_{10}$ (see Scheme SI-1).

(ii) for additional 80 ps, time step was increased to 0.4 fs and put in contact with a heat bath simulated using Lowe-Andersen thermostat with a collision rate of 1 fs^{-1}. To obtain an amorphous silica glass, the sample was subsequently gradually cooled down to 300 K at a rate of 0.01 K/0.5 fs for 185 ps and equilibrated for additional 100 ps at 300 K. A 10 ns equilibration was performed before a production run of 1 ns for subsequent characterization of the amorphous sample.

The pair radial distribution functions $g_{ij}(r)$ were computed and are in close agreement with the X-Ray diffraction measurements (in orange) from Mozzi *et al.*[S4], as shown in Figure SI-3. From the integral to the first minimum of $g_{ij}(r)$ one can determine a coordination number of 3.93 and 1.96 for the Si and O atoms, respectively (expected 4 and 2, respectively). A

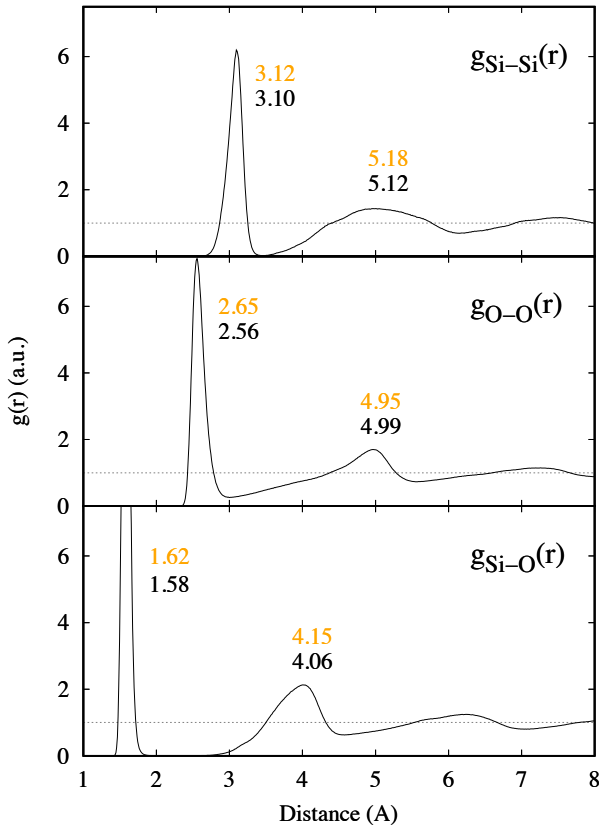

Figure SI-3: Radial distribution functions $g(r)$ for Si–Si pairs (top), O-O pairs (middle) and Si-O pairs (bottom), computed at 300 K for amorphous silica. Experimental (orange) distances[S4] are shown for each peak together with theoretical values (black).

glass surface was then obtained using an approach similar to that described by Feuston and

Garofalini[S5]. The simulation box was extended to 150 Å in the z direction, rendering the periodic boundary conditions effective only in the x and y directions for the resulting SiO_2 slab and a 20 Å-thick layer of atoms was kept immobile at the bottom (Figure SI-4). The free surface was annealed at 1000 K for 1 ns to mimic the spontaneous heating during the fracture, as well as to help the local surface reconstruction and structure relaxation. The sample was then gradually cooled down to 300 K at a rate of 0.02 K/fs and further relaxed for 5 ns. Based on the assumption that the grafted molecules link to the surface via a Si-

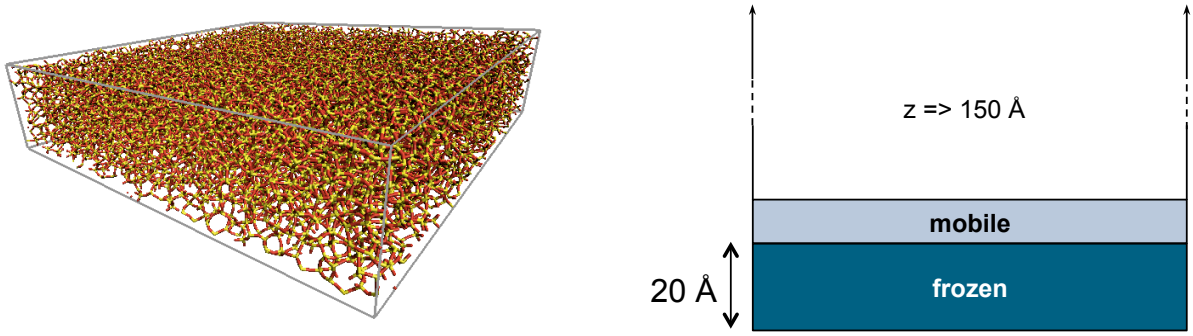

Figure SI-4: Equilibrated bulk of amorphous SiO_2 (left), and sketch of the simulation box used for the SiO_2 surface (right).

O single bond, one hydroxyl hydrogen of the -Si-$(OH)_3$ group was removed and its charge summed to the one of the corresponding oxygen atom. The surface was prepared for grafting as follows: oxygen atoms with coordination number of 1 located at $z > 27$ Å were removed from the slab and the corresponding total charge redistributed over the atoms of the frozen layer ($z \leq 20$ Å). A specific Lennard-Jones interaction ($\epsilon = -0.1554$ kcal/mol, $r = 1.64$ Å) was then added between alkylsilane grafting oxygens and "reactive" silicon atoms from the surface (the ones previously bonded to monocoordinate oxygen atoms), providing an effective bond without explicit grafting.[S6]

Functionalized surfaces with various coverage rates

After the preparation of a fully covered azidoalkyl SAM, only a fraction of the azide groups was substituted by chromophore units, with the rationale of avoiding a too close packing of the chromophores onto the surface that could hamper the efficiency of the switching process. Three samples with different relative chromophore fraction (1/4, 1/2 and 3/4) were generated, corresponding to coverages of 1.13, 2.26 and 3.38 molecules/nm^2, respectively. As can be seen in Figure SI-5, decreasing the coverage induces a decrease of the SAM thickness, evaluated as the average difference between the height of the complete system and that of the SiO_2 surface alone. The numerical data are collected in Table SI-1.

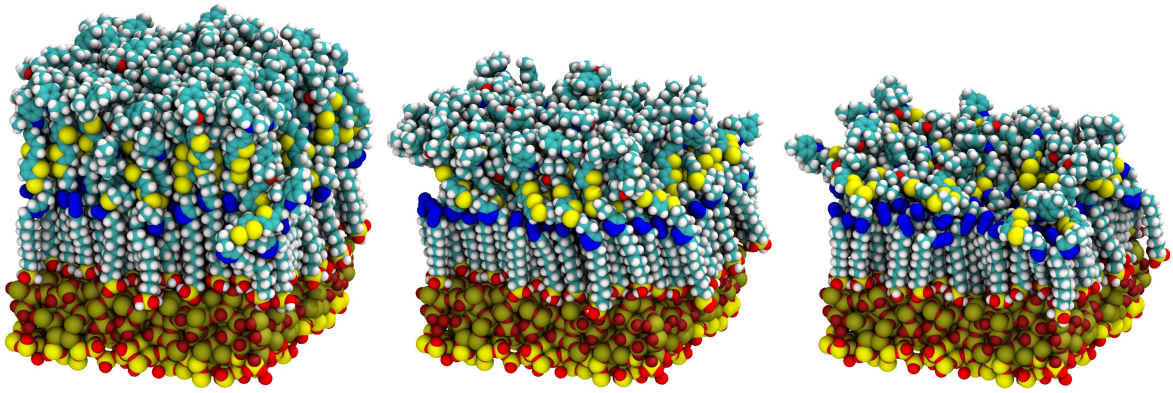

Figure SI-5: From left to right: SAMs functionalized with the closed IND molecule, with relative grafting ratios of 1/4, 1/2 and 3/4.

Table SI-1: Average value of the cosine of the tilt angle, θ_{tilt}), defined as the angle between the double C-C bond of the vinyl bridge (red segment in Fig. SI-1) and the axis normal to the surface plane. Thickness and roughness (both in Å) of the SAM in its closed form (CF) and in its open form (OF), with respect to the relative coverage (1/4, 1/2 or 3/4).

Property	CF (1/4)	CF (1/2)	CF (3/4)	OF (3/4)
$\cos^2(\theta_{tilt})$	0.220	0.396	0.362	0.448
Thickness	26.68	33.96	40.40	40.56
Roughness	3.15	2.03	1.32	1.44

Choice of the relevant molecular fragment for NLO calculations

Before running NLO calculations on molecular structures extracted from MD simulations, preliminary tests were carried out to define the size of the fragments that should be considered. The complete reference molecule (IND1 in Figure SI-6), including from the indolino-oxazolidine photoresponsive part to the terminal $Si(OH)_3$ anchoring unit was first optimized at the M06/6-311G(d) level, and its first hyperpolarizability β subsequently calculated at the M06-2X/6-311G(d) level. Then, the NLO properties of the simplified fragments illustrated in Figure SI-6 were calculated at the same level of theory, without performing any further geometrical relaxation. So, in the IND2 fragment, the $Si(OH)_3$ anchor was removed and replaced by an hydrogen atom; starting from IND2, the alkyl chain was removed in IND3 and replaced by a simple methyl group; finally, the triazole moiety as well as the central $(CH_2)_3$ chain were removed and replaced by a methyl group in IND4. The geometries of the refer-

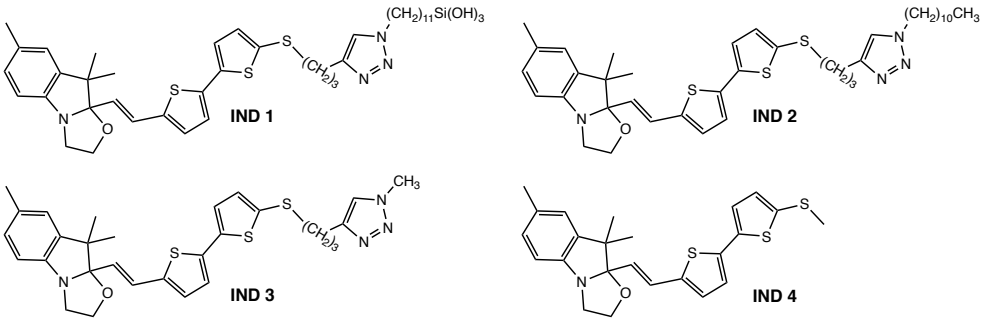

Figure SI-6: Molecular fragments considered in DFT calculations of the NLO properties.

ence open and closed conformers are illustrated in Figure SI-7, and the relevant geometrical parameters are gathered in Table SI-2. The β values calculated for the four IND 1-4 systems in both their closed and open forms are collected in Table SI-3. According to a previous study on indolino-oxazolidine molecules in solution (corresponding to the IND4 system),[S7] one single conformer exists at room temperature for the closed form, while three conformers differing by the values of the θ_7 and θ_9 dihedrals exhibit non negligible populations for the open form. The corresponding three conformers were therefore considered as starting struc-

tures for geometry optimizations of the OF in the present study. The static and dynamic

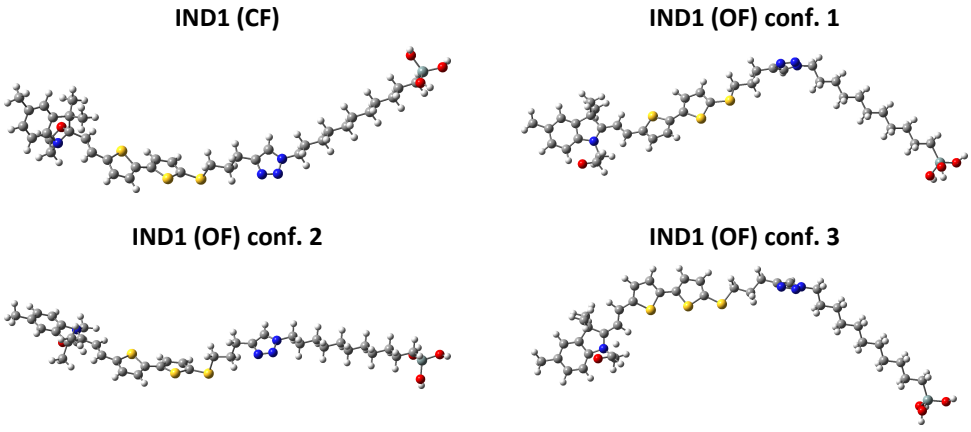

Figure SI-7: Geometry of the reference IND1 molecules optimized at the M06/6-311G(d) level.

hyperpolarizabilities of the closed form (CF) and open form (OF) of the four systems defined in Figure SI-6 are collected in Table SI-3, while the $\beta(OF)/\beta(CF)$ contrast ratios are reported in Table SI-4. The results lead to similar conclusions for the static and dynamic cases. With the exception of the relatively large ∼10% error obtained for the dynamic β of the conformer 3 (IND2 OF), removing the terminal $Si(OH)_3$ anchoring unit neither impacts the β values, which deviate from the reference ones by $< 4\%$ for the CF and $< 1\%$ for the OF, nor the OF/CF contrasts, for which the errors are smaller than 5%. Removing the alkyl chain induces slightly larger errors on the β values of both CF and OF, but the latter remain lower than 10%, again with the exception of the dynamic value of conformer 3 (IND3 OF), which reaches 22%. Finally, the most simplified IND4 system leads to large errors on β, of the order of 60% for the CF and ranging from 22% to 47% for OF; in addition OF/CF contrasts are significantly overestimated. On the basis of these results, the IND2 fragment was selected as the best trade-off between accuracy and calculation time for all further DFT calculations of the NLO properties of the photochromic molecules extracted from the MD simulation trajectory.

Table SI-2: Bond Length Alternation (BLA, Å) along the vinyl bridge of the indolino-oxazolidine moiety (red segment in Fig. SI-1, and torsional angles (θ_{5-9} and γ, degrees) calculated at the M06/6-311G(d) level for the reference system (IND1) defined in Figure SI-6 in its closed and open form (CF, OF). Three different conformers are considered for the OF.

System (form)	Conf.	BLA	θ_4	θ_5	θ_6	γ
IND1 (CF)	1	-0.135	158.1	1.2	-17.7	101.7
System (form)	Conf.	BLA	θ_7	θ_8	θ_9	γ
IND1 (OF)	1	-0.051	-167.1	-5.9	-24.9	-16.4
IND1 (OF)	2	-0.055	158.5	2.5	-174.6	99.8
IND1 (OF)	3	-0.053	-25.8	3.3	-173.2	7.1

Table SI-3: Static ($\lambda = \infty$) and dynamic ($\lambda = 1064$ nm) hyperpolarizabilities (β, a.u.) calculated at the M06-2X/6-311G(d) level for the four systems defined in Figure SI-6 in their closed and open form. Three conformers (Conf.) are considered for the open forms. The relative differences (% Diff.) between the β values calculated for the IND2-4 systems and the reference IND1 system are also reported. All β values are given in atomic units (1 au of $\beta = 3.6310^{-42}$ $\mathbf{m}^4\mathbf{V}^{-1} = 3.2063 \times 10^{-53}$ $\mathbf{C}^3\mathbf{m}^3\mathbf{J}^{-2} = 8.641 \times 10^{-33}$ esu).

		$\lambda = \infty$		$\lambda = 1064$ nm	
System (form)	Conf.	β	% Diff.	β	% Diff.
IND1 (CF)	1	846	/	1306	/
IND2 (CF)	1	878	3.66	1325	1.45
IND3 (CF)	1	797	-5.90	1193	-8.65
IND4 (CF)	1	334	-60.57	468	-64.17
System (form)	Conf.	β	% Diff.	β	% Diff.
IND1 (OF)	1	13668	/	114016	/
IND2 (OF)	1	13572	-0.70	113328	-0.60
IND3 (OF)	1	12766	-6.60	109830	-3.67
IND4 (OF)	1	8967	-34.39	89040	-21.91
IND1 (OF)	2	3961	/	27787	/
IND2 (OF)	2	3965	0.10	25094	-9.69
IND3 (OF)	2	3941	-0.50	21669	-22.02
IND4 (OF)	2	4974	25.57	14777	-46.82
IND1 (OF)	3	13731	/	49260	/
IND2 (OF)	3	13778	0.34	48435	-1.67
IND3 (OF)	3	13147	-4.25	45833	-6.96
IND4 (OF)	3	9547	-30.47	33966	-31.05

Table SI-4: $\beta(OF)/\beta(CF)$ **contrast ratios for the static** ($\lambda = \infty$) **and dynamic** ($\lambda = 1064$ **nm) first hyperpolarizabilities, calculated at the M06-2X/6-311G(d) level for the four systems defined in Figure SI-6 (considering three different conformers (Conf.) for the OF). The relative differences (% Diff.) between the contrast values calculated for the IND2-4 systems and the reference IND1 system are also reported.**

		$\lambda = \infty$		$\lambda = 1064$ nm	
System	Conf.	$\beta(OF)/\beta(CF)$	% Diff.	$\beta(OF)/\beta(CF)$	% Diff.
IND1	1	16.14	/	87.30	/
IND2	1	15.46	-4.21	85.53	-2.03
IND3	1	16.02	-0.74	92.06	5.45
IND4	1	26.85	66.37	190.26	117.93
IND1	2	4.68	/	21.28	/
IND2	2	4.52	-3.43	18.94	-10.99
IND3	2	4.94	5.74	18.16	-14.63
IND4	2	14.89	218.45	31.57	48.40
IND1	3	16.21	/	37.72	/
IND2	3	15.69	-3.20	36.55	-3.08
IND3	3	16.50	1.75	38.42	1.86
IND4	3	28.58	76.32	72.58	92.42

Probability distributions of dihedrals

Figures SI-8 and SI-9 report the potential energy curves associated to torsions within the isolated molecule around the $\theta_1 - \theta_{10}$ and $\gamma - \gamma'$ dihedrals, respectively. The plots also show the probability distributions of the dihedral angles for the subset of molecular geometries extracted from the MD trajectories. The distributions indicate that the θ_2 and θ_3 (and in a lesser extent θ_1) dihedrals assume all possible values due to low rotational energy barriers, while all other dihedrals ($\theta_4 - \theta_{10}$) adopt specific values due to larger energy barriers associated to steric and conjugation constraints.

Relationships between geometrical structures and NLO responses

Figures SI-10 and SI-11 report the scatter plots of β with respect to torsions around $\theta_1 - \theta_{10}$ and $\gamma - \gamma'$ dihedrals, respectively. These graphs evidence how the amplitude of the NLO responses of the molecules within the SAM is strongly correlated to the value of the γ dihedral: large β values are obtained when γ is close to 0° or 180°, while β is much weaker when γ is close to 90°. To gain further insights on the $\gamma - \beta$ relationship, we focused on the three open-form conformers of IND2, since this molecular fragment was selected for the statistical sampling of the NLO properties. As reported in Table SI-3, conformers 1 and 3 display very similar static β values associated to quasi planar conformations with respect to γ, while conformer 2 exhibits a much lower β value associated to a perpendicular conformation. Within the two-state approximation (TSA), the static first hyperpolarizability of these conformers can be expressed as:

$$\beta^{TSA} = 6 \times \frac{\mu_{ge}^2 \Delta\mu_{ge}}{\Delta E_{ge}} = 9 \times \frac{f_{ge} \Delta\mu_{ge}}{\Delta E_{ge}^2} \qquad \text{(SI-1)}$$

in which ΔE_{ge} is the excitation energy between the ground state (g) and the dipole-allowed excited state (e), μ_{ge} is the transition dipole associated to the excitation, $f_{ge} = \frac{2}{3}\Delta E_{ge}\mu_{ge}^2$ is the oscillator strength, and $\Delta\mu_{ge} = |\overrightarrow{\mu_e} - \overrightarrow{\mu_g}|$ is the change in dipole moment between the

two electronic states. This latter quantity can be factorized into two contributions:

$$\Delta\mu_{ge} = \Delta q \times \Delta r \tag{SI-2}$$

where Δq is the amount of charge transferred during the excitation, and Δr is the average distance over which this charge transfer occurs. The quantities involved in equations SI-1 and SI-2 were calculated for the three lowest-energy excitations of the IND2 open-form conformers using time-dependent DFT at the M06-2X/6-311G(d) level, and are collected in Table SI-5. Results show that S_2 and S_3 exhibit strong optical absorption (with large oscillator strengths f_{ge}), while the $S_0 \rightarrow S_1$ transition is dipole forbidden with f_{ge} close to zero. Thus, according to equation SI-1, the dark S_1 state does not contribute to the second-order response of the compounds. The differences in the total densities of the optically active S_2 and S_3 states and ground state are reported in Figure SI-12. The density maps show that the lowest-energy $S_0 \rightarrow S_2$ transition is localized on the indolino-oxazolidine moiety and the closest thiophene ring, with no contribution of the central sulfur atom. The most intense $S_0 \rightarrow S_3$ transition is more delocalized and induces an electronic redistribution impacting both the indolino-oxazolidine and bithiophene units. Moreover, in conformers 1 and 3 (showing quasi planar conformations with respect to γ), the charge transfer extends to the central sulfur atom, while this latter does not contribute to the density reorganization in conformer 2 (showing a perpendicular conformation with respect to γ). Therefore, the excitation-induced charge transfer is much more pronounced in planar conformers 1 and 3, with dipole moment variations $\Delta\mu_{ge}$ two times larger than that of conformer 2, mainly due to an increase of the charge transfer distance Δr. In addition, the $S_0 \rightarrow S_3$ transition energies of conformers 2 and 3 are lower than that of conformer 2, which also contributes to increase the β values of these two conformers with respect to conformer 2. The dependence of β on the value of the dihedral angle γ is then explained in terms of the sizable participation of the sulfur atom of the thioalkyl group to the brightest S_3 excitation in the case of planar conformers,

as highlighted in Figure SI-12.

Table SI-5: Excitation energies (ΔE_{ge}, eV), oscillator strengths (f_{ge}), dipole moment variation ($\Delta\mu_{ge}$, D), charge transfer (Δq, |e|) and charge transfer distance (Δr, Å) for the three lowest-energy excitations of the three IND2 open-form conformers.

System (form)	Conf.	Transition	ΔE_{ge}	f_{ge}	$\Delta\mu_{ge}$	Δq	Δr
IND2 (OF)	1	$S_0 \rightarrow S_1$	1.3908	0.0010	9.605	1.013	1.974
		$S_0 \rightarrow S_2$	1.7878	0.3598	3.203	0.470	1.418
		$S_0 \rightarrow S_3$	2.8953	1.2107	7.289	0.538	2.822
IND2 (OF)	2	$S_0 \rightarrow S_1$	1.4396	0.0069	8.194	0.951	1.794
		$S_0 \rightarrow S_2$	1.9202	0.4573	1.548	0.383	0.841
		$S_0 \rightarrow S_3$	3.1123	1.1350	3.774	0.478	1.644
IND2 (OF)	3	$S_0 \rightarrow S_1$	1.4528	0.0043	7.171	0.946	1.578
		$S_0 \rightarrow S_2$	1.8864	0.4223	1.628	0.388	0.874
		$S_0 \rightarrow S_3$	2.9850	1.0865	7.735	0.559	2.879

Origin of the resonance enhancement of the first hyperpolarizability of open forms

To gain insight on the origin of the huge resonance enhancement of the first hyperpolarizability observed for few structures extracted from the open-form SAM layer, the absorption properties of molecules exhibiting the lowest and the largest dynamic β values (respectively referred to as **1** and **2** in the following) were calculated at the M06-2X/6-311G(d) level. The vertical excitation energies and oscillator strengths associated to the lowest-energy optical transitions are reported in Table SI-6 for these two chromophore geometries. Structure **1** with minimal β displays an intense absorption transition ($S_0 \rightarrow S_3$) at 449 nm, as well as a transition ($S_0 \rightarrow S_2$) at 582 nm, associated to a lower oscillator strength. In structure **2** displaying the maximal dynamic β value, the absorption wavelength of the lowest-energy optically-absorbing excited state (S_3) is associated to the largest oscillator strength and red-shifted to 546 nm, *i.e.* very close to the second harmonic wavelength of a 1064 nm laser. This state is thus at the origin of the large resonance-enhancement of the first hyperpolarizability

in this structure.

Table SI-6: Excitation energies (ΔE_{ge}, eV), wavelengths (λ_{ge}, nm) and oscillator strengths (f_{ge}) associated to the lowest-energy dipole-allowed excitations of the open-form molecular structures exhibiting the lowest (1) and largest (2) dynamic β values (in a.u.).

Structure	β	Transition	ΔE_{ge}	λ_{ge}	f_{ge}
1	3295	$S_0 \rightarrow S_2$	2.1302	582	0.3611
		$S_0 \rightarrow S_3$	2.7585	449	0.8995
		$S_0 \rightarrow S_5$	3.6252	342	0.1236
2	$>10^{11}$	$S_0 \rightarrow S_3$	2.2718	546	0.8026
		$S_0 \rightarrow S_4$	2.9335	423	0.3023
		$S_0 \rightarrow S_5$	3.2863	377	0.2020

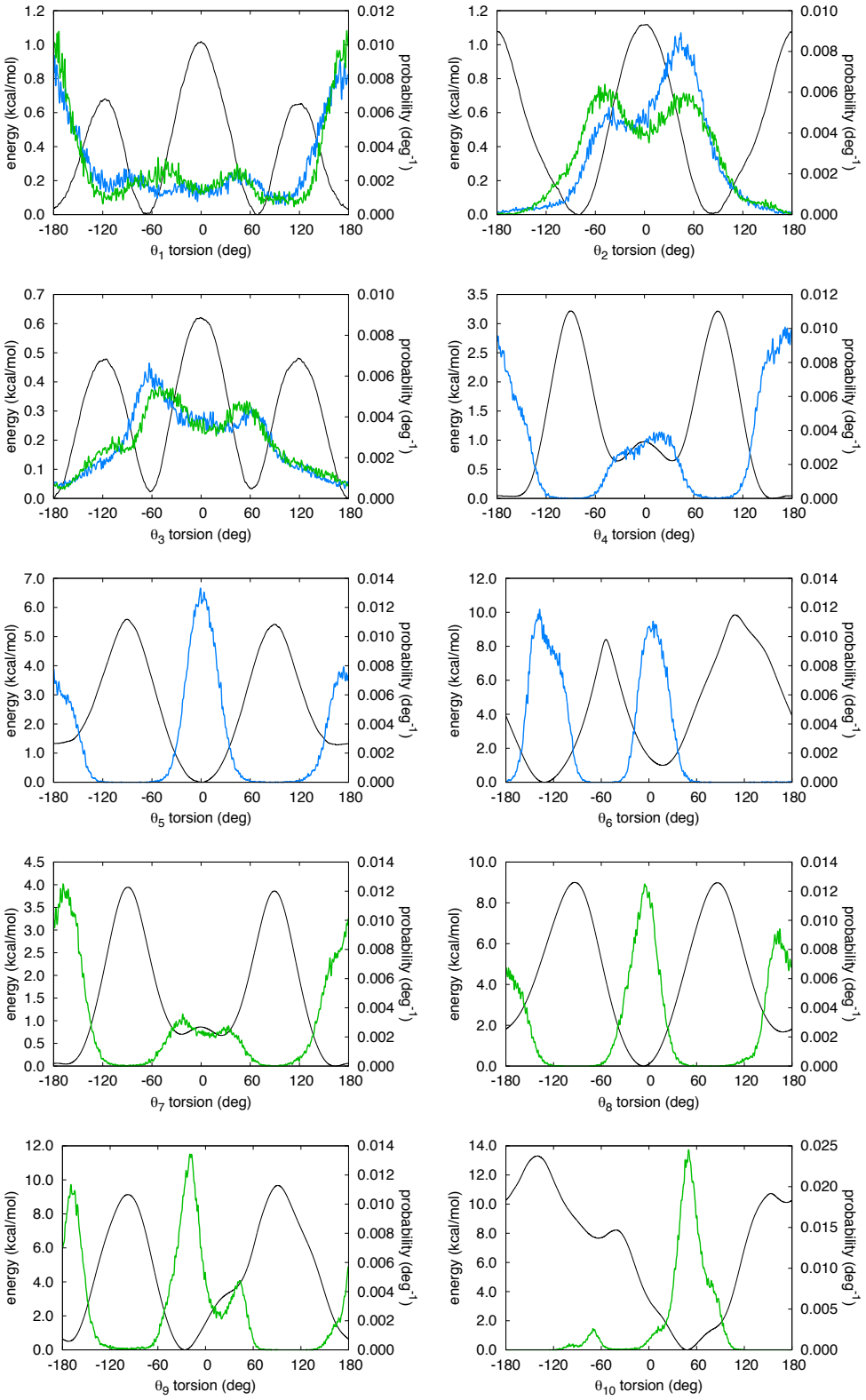

Figure SI-8: Potential energy curves associated to torsions $\theta_1 - \theta_{10}$ (black line) and probability distributions of the dihedral angles of molecules in the SAM, in the closed (blue) and open (green) forms.

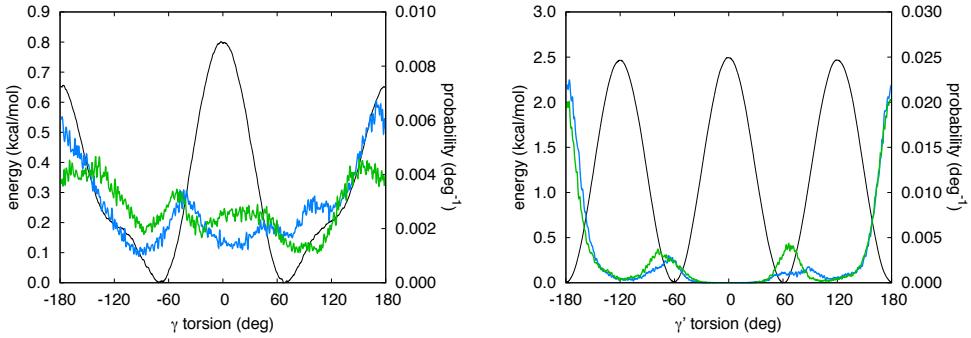

Figure SI-9: Potential energy curves associated to torsions γ and γ' (black line) and probability distributions of the dihedral angles of molecules in the SAM, in the closed (blue) and open (green) forms.

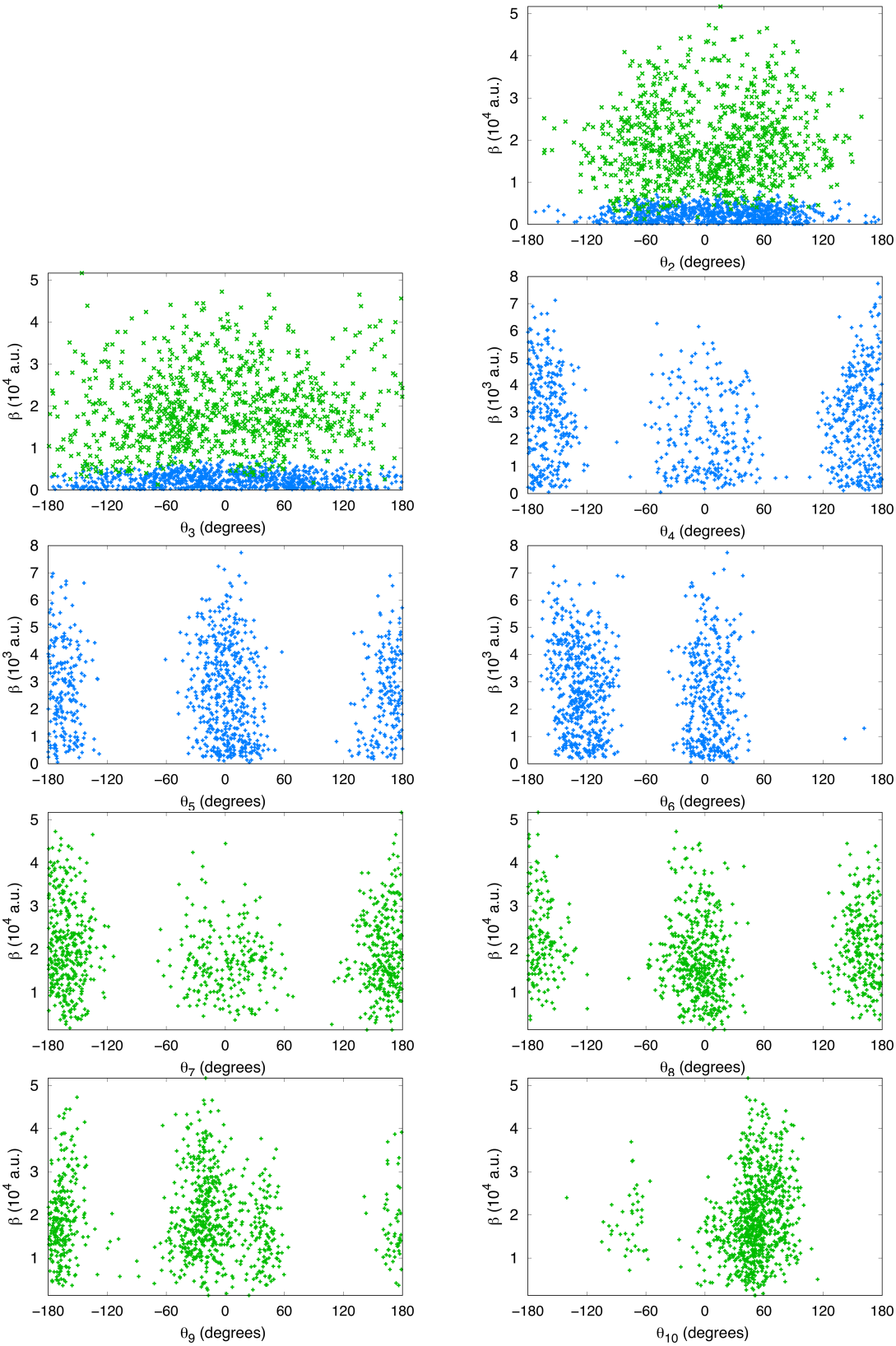

Figure SI-10: Scatter plots of individual values of β with respect to torsion angles $\theta_2 - \theta_{10}$ for molecules in closed (blue) and open (green) forms.

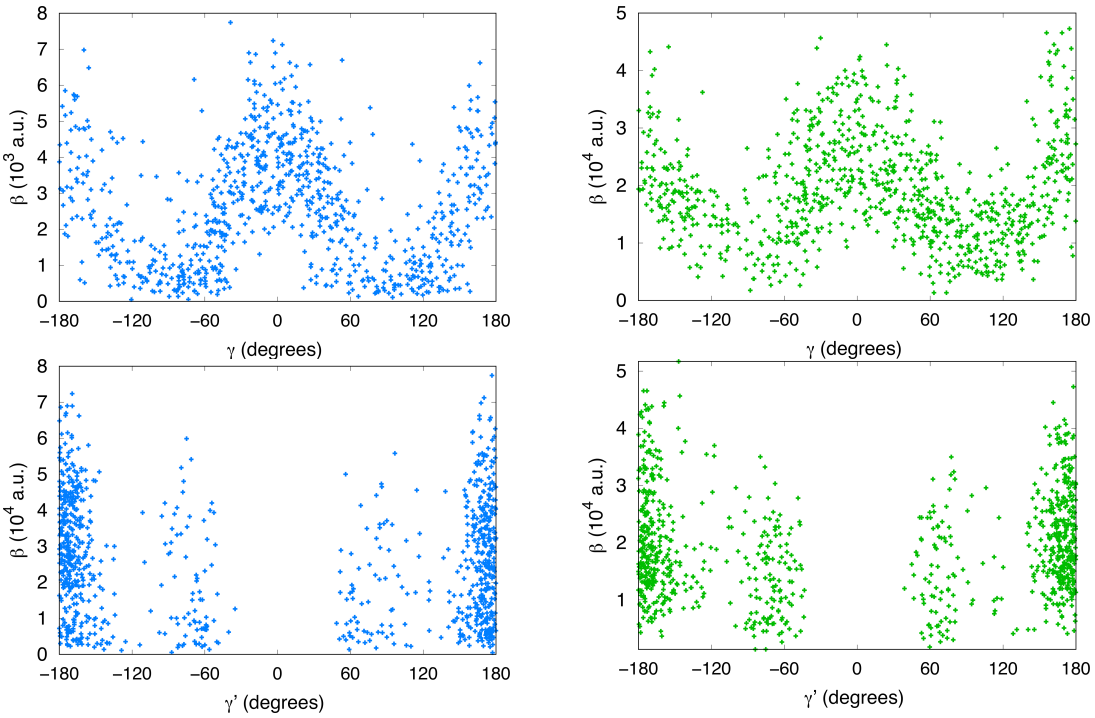

Figure SI-11: Scatter plots of individual values of β with respect to torsion angles γ and γ' for molecules in closed (blue) and open (green) forms.

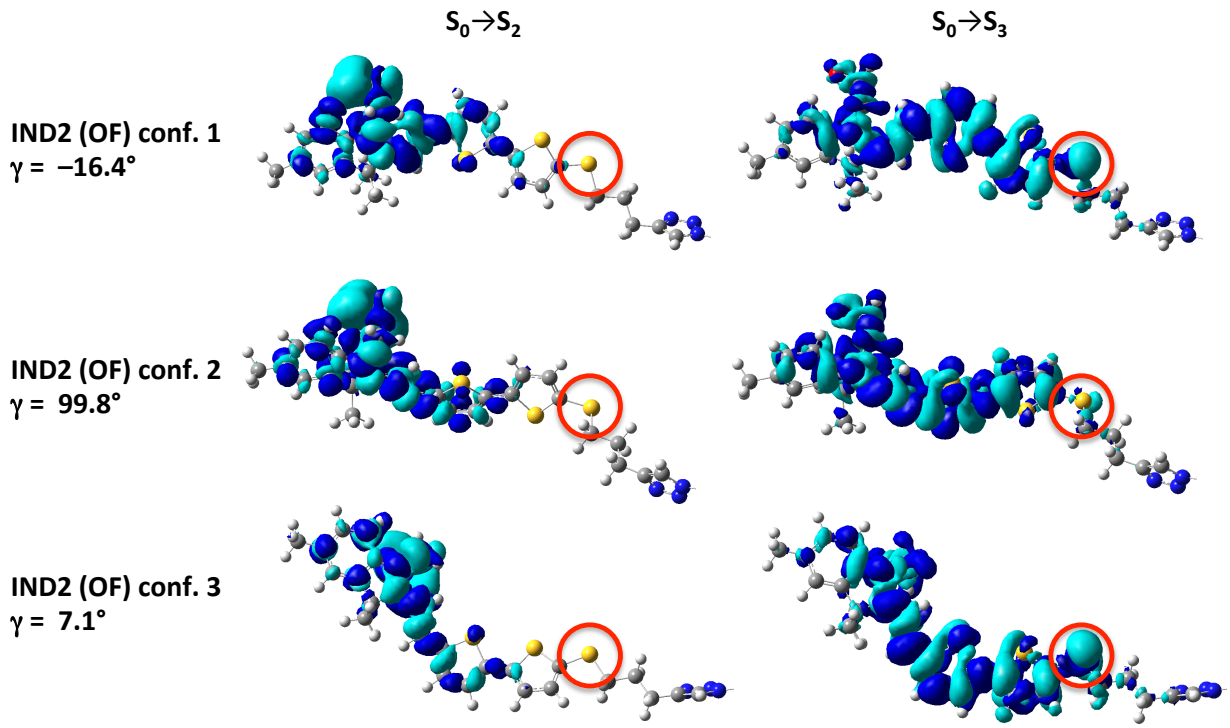

Figure SI-12: Density difference maps calculated at the M06-2X/6-311G(d) for the three IND2 open-form conformers (isovalues = 0.0004). Light (dark) blue lobes are associated with negative (positive) values. The terminal alkyl chains are hidden for clarity. The red circles highlight the contribution of the thioalkyl sulfur atom in the electronic redistribution.

References

(S1) Cygan, R. T.; Liang, J.-J.; Kalinichev, A. G. Molecular Models of Hydroxide, Oxyhydroxide, and Clay Phases and the Development of a General Force Field. *J. Phys. Chem. B* **2004**, *108*, 1255–1266.

(S2) Valle, R. G. D.; Andersen, H. C. Molecular dynamics simulation of silica liquid and glass. *J. Chem. Phys.* **1992**, *97*, 2682–2689.

(S3) Martínez, L.; Andrade, R.; Birgin, E. G.; Martínez, J. M. PACKMOL: A package for building initial configurations for molecular dynamics simulations. *J. Comput. Chem.* **2009**, *30*, 2157–2164.

(S4) Mozzi, R. L.; Warren, B. E. The structure of vitreous silica. *J. Appl. Crystallogr.* **1969**, *2*, 164–172.

(S5) Feuston, B. P.; Garofalini, S. H. Topological and bonding defects in vitreous silica surfaces. *J. Chem. Phys.* **1989**, *91*, 564–570.

(S6) Mityashin, A.; Roscioni, O. M.; Muccioli, L.; Zannoni, C.; Geskin, V.; Cornil, J.; Janssen, D.; Steudel, S.; Genoe, J.; Heremans, P. Multiscale Modeling of the Electrostatic Impact of Self-Assembled Monolayers used as Gate Dielectric Treatment in Organic Thin-Film Transistors. *ACS Appl. Mater. Interfaces* **2014**, *6*, 15372–15378.

(S7) Pielak, K.; Bondu, F.; Sanguinet, L.; Rodriguez, V.; Champagne, B.; Castet, F. Second-Order Nonlinear Optical Properties of Multiaddressable Indolinooxazolidine Derivatives: Joint Computational and Hyper-Rayleigh Scattering Investigations. *J. Phys. Chem. C* **2017**, *121*, 1851–1860.

Atomic coordinates of the reference IND1 molecule

IND1 closed form

C	11.06435100	1.94829900	-0.62034400
C	10.51681700	2.98303200	0.13306200
C	11.13203500	4.21461700	0.17974200
C	12.32284600	4.43231900	-0.52165400
C	12.85276900	3.38438000	-1.26597100
C	12.23609800	2.13692300	-1.32962700
H	10.69989800	5.02589200	0.76907700
H	13.77868700	3.54431900	-1.81761400
H	12.66825200	1.34060200	-1.93275200
C	12.99854400	5.76815000	-0.46436800
H	12.35565800	6.56455800	-0.85942000
H	13.25364300	6.04874600	0.56500200
H	13.92567300	5.77761600	-1.04618400
C	9.21499900	2.52271400	0.73547800
C	9.00570500	2.94531800	2.17879100
H	8.88572100	4.03366800	2.24213100
H	8.09379200	2.49416100	2.58996600
H	9.84610600	2.64833700	2.80951900
C	8.06750400	3.04181100	-0.13122600
H	8.15718100	2.70217800	-1.16918900
H	7.09276900	2.71405800	0.24873600
H	8.07990900	4.13820100	-0.13531000
C	9.37076800	0.98196900	0.58917100
C	8.08752000	0.22043200	0.49588700
H	7.57088800	0.11205700	1.45243200
C	7.58382000	-0.30399700	-0.62171300
H	8.14477300	-0.16733400	-1.55003800
C	6.35289900	-1.04405500	-0.75520200
C	5.84844400	-1.58620600	-1.90788100
S	5.27921100	-1.35179100	0.58318300
C	4.62274800	-2.25828500	-1.73162500
H	6.36640000	-1.50307500	-2.85978300
C	4.17301200	-2.23359800	-0.43774700
H	4.09008600	-2.76923400	-2.52915800
C	2.97142600	-2.80888600	0.11472700
C	2.69961400	-3.13295900	1.41992500
S	1.61049600	-3.17927100	-0.90580000
C	1.40827100	-3.66892500	1.60878600
H	3.42477000	-3.00324000	2.21910600
C	0.68657200	-3.76355100	0.45258800
H	1.00876800	-3.99104400	2.56589800
S	-0.93681700	-4.40045900	0.24824100
C	-1.87017100	-2.82148400	0.13980400
H	-1.63678100	-2.22768300	1.03213000
H	-1.51761000	-2.26716300	-0.73876900
C	-3.35167400	-3.10978800	0.03935400
H	-3.56130200	-3.73766200	-0.83676500
H	-3.68531000	-3.68189600	0.91703700
C	-4.16390200	-1.82361800	-0.07101100
H	-3.98415500	-1.18822800	0.80754100
H	-3.81508100	-1.25213000	-0.94337000
C	-6.66024400	-1.80380400	0.63512600
H	-6.71635600	-1.31557200	1.59865400
C	-5.61973900	-2.08567600	-0.21224400
N	-6.12918400	-2.72220700	-1.29989600
N	-7.41227500	-2.84067500	-1.16858100
N	-7.75093100	-2.29647000	0.00674600

C	-9.14744200	-2.17661100	0.37692600
H	-9.66637000	-3.01966800	-0.09215000
H	-9.22644800	-2.30159500	1.46442700
C	-9.73857600	-0.85415100	-0.07048900
H	-9.61141700	-0.76682600	-1.15916400
H	-9.15908500	-0.02930400	0.37241200
C	-11.20202800	-0.71970500	0.30429400
H	-11.77507300	-1.54947800	-0.13965600
H	-11.31752700	-0.82937600	1.39507200
C	-11.80093200	0.60297700	-0.13612200
H	-11.21765600	1.43051200	0.29937300
H	-11.69140400	0.70835800	-1.22726600
C	-13.26107200	0.76218000	0.24414100
H	-13.84841700	-0.05926300	-0.19738500
H	-13.37041600	0.64967600	1.33521300
C	-13.84691700	2.09347000	-0.18721500
H	-13.25206400	2.91243600	0.24923600
H	-13.74201000	2.20415800	-1.27870700
C	-15.30349200	2.26915800	0.19988600
H	-15.90263400	1.45731400	-0.24388400
H	-15.40955500	2.15089300	1.29071300
C	-15.87651700	3.60959700	-0.22037300
H	-15.27399300	4.41962200	0.22195400
H	-15.77196100	3.72830500	-1.31109900
C	-17.33110500	3.79553700	0.16897000
H	-17.93885300	2.99272400	-0.27995300
H	-17.43917400	3.67286300	1.25928500
C	-17.89179600	5.14451300	-0.24311400
H	-17.28622100	5.94598000	0.20476700
H	-17.78579900	5.26796900	-1.33204800
C	-19.35399200	5.33402500	0.14886200
H	-19.95802000	4.55271900	-0.31245300
H	-19.45009700	5.27508300	1.23301500
C	10.95882600	-0.46192900	-0.24736300
H	11.91443700	-0.51592600	-0.77440600
H	10.34540000	-1.31089300	-0.56623900
C	11.10511600	-0.41091700	1.27560200
H	12.08360800	-0.00622300	1.57106500
H	10.97892000	-1.39545400	1.74247200
O	10.09294900	0.47070000	1.72153600
N	10.26203200	0.78287400	-0.55352700
H	-19.69853100	6.30967200	-0.19392900

IND1 open form, conformer 1

C	11.59577700	1.28003600	-0.84863100
C	11.63100600	-0.00716800	-1.36006100
C	12.81436800	-0.52135400	-1.84480700
C	13.96881500	0.26595100	-1.80108200
C	13.90125500	1.54289700	-1.24108900
C	12.71803500	2.08203400	-0.75153400
H	12.86238500	-1.53441800	-2.24712700
H	14.81468600	2.13118900	-1.16910600
H	12.67385700	3.02548100	-0.21109800
C	15.26051600	-0.25453000	-2.35049200
H	15.33862500	-1.34186800	-2.24439000
H	15.35703100	-0.02822400	-3.42020300
H	16.12351800	0.19412000	-1.84826700
C	10.26785200	-0.62277500	-1.22545100
C	9.67001400	-0.92942100	-2.60095400
H	10.29426800	-1.66660200	-3.11905500

H	8.65985000	-1.34734100	-2.52129500
H	9.62384800	-0.02985300	-3.22439100
C	10.30348800	-1.88003200	-0.35910700
H	10.72290500	-1.66604700	0.62937600
H	9.29998000	-2.29932100	-0.22261100
H	10.92724100	-2.64682200	-0.83354700
C	9.49720600	0.49718800	-0.54695100
C	8.14178500	0.36145700	-0.17962700
H	7.62841700	-0.46744500	-0.67244700
C	7.44499300	1.06630300	0.75802400
H	7.97143000	1.78521600	1.38552800
C	6.07737100	0.88914400	1.09506000
C	5.40777900	1.51361400	2.12661400
S	4.99756000	-0.19225300	0.24083200
C	4.06994200	1.12265500	2.25372700
H	5.90019700	2.22931600	2.77926400
C	3.67980000	0.19169900	1.31681500
H	3.40132400	1.49409900	3.02516900
C	2.39903100	-0.43408500	1.15390200
C	2.05582000	-1.52213800	0.39585000
S	0.99451300	0.18206300	1.99868800
C	0.69757000	-1.88888200	0.49835700
H	2.77548200	-2.07048900	-0.20662200
C	-0.01171700	-1.07293400	1.33880800
H	0.26678300	-2.73978300	-0.01849800
S	-1.69337000	-1.11648100	1.82688100
C	-2.37864100	-2.21912700	0.54726200
H	-2.07842600	-1.83655600	-0.43668100
H	-1.95525100	-3.22341000	0.67426500
C	-3.88633500	-2.26041900	0.68579300
H	-4.16959700	-2.61578700	1.68504300
H	-4.30201100	-1.24822100	0.58558500
C	-4.51541700	-3.17818700	-0.35635100
H	-4.28550800	-2.81581500	-1.36810100
H	-4.06527800	-4.17852500	-0.27514300
C	-7.01493000	-2.94313900	-1.02071700
H	-7.04662900	-2.51322500	-2.01269000
C	-5.98722400	-3.29102200	-0.18230300
N	-6.53047400	-3.79995700	0.95465100
N	-7.82168700	-3.78684200	0.85852500
N	-8.13337000	-3.27773200	-0.33937100
C	-9.52179800	-3.06938500	-0.70203800
H	-9.62794200	-3.26614600	-1.77651600
H	-10.09770700	-3.83295800	-0.16781700
C	-10.00717800	-1.67721700	-0.34817700
H	-9.38200400	-0.92990400	-0.86076200
H	-9.85701100	-1.51701100	0.72909700
C	-11.46524100	-1.47790200	-0.71562300
H	-11.60414800	-1.66544500	-1.79300900
H	-12.08056000	-2.23387800	-0.20188100
C	-11.98188400	-0.09204900	-0.37594600
H	-11.84890800	0.09497200	0.70149900
H	-11.36441300	0.66506800	-0.88583600
C	-13.43871400	0.10703200	-0.75000700
H	-13.56932400	-0.08680400	-1.82725400
H	-14.05536800	-0.64948500	-0.23798000
C	-13.96296600	1.49229000	-0.42048000
H	-13.83845000	1.68591300	0.65724000
H	-13.34417000	2.24944500	-0.92911900
C	-15.41774400	1.68823800	-0.80444000

H	-15.54097400	1.49085700	-1.88194900
H	-16.03657600	0.93196300	-0.29440800
C	-15.94652200	3.07347300	-0.48204500
H	-15.82844700	3.27074600	0.59574700
H	-15.32646800	3.83051600	-0.98924900
C	-17.39942700	3.26737300	-0.87361000
H	-17.51876000	3.07058900	-1.95179000
H	-18.02198000	2.51265400	-0.36541400
C	-17.92808800	4.65369400	-0.55250900
H	-17.81318700	4.85114700	0.52352200
H	-17.30739700	5.40875400	-1.05946600
C	-19.38840400	4.84575300	-0.95104400
H	-19.49940800	4.67251800	-2.03163100
H	-20.01625300	4.13108800	-0.39872100
C	9.93610500	2.87203200	0.06358300
H	8.85297500	3.01321900	-0.00917100
H	10.45139100	3.61666200	-0.55003400
C	10.44288400	3.12521600	1.58929800
H	9.90617700	2.30575900	2.16100000
H	9.87120800	4.07506300	1.81418300
O	11.72275000	3.16422600	1.69757900
N	10.27475100	1.57567100	-0.42870400
H	-19.70230200	5.87210900	-0.71008600

IND1 open form, conformer 2

C	11.15614100	1.49734900	-1.24424800
C	11.61169200	0.22719800	-0.93712400
C	12.91649500	-0.12676600	-1.21347200
C	13.76807900	0.80758100	-1.80280800
C	13.28480000	2.09123900	-2.07225600
C	11.98057700	2.46384000	-1.79414200
H	13.29116000	-1.12070200	-0.96605700
H	13.96497000	2.82723900	-2.49858100
H	11.64350400	3.48007500	-1.96020600
C	15.18296500	0.45525200	-2.14084500
H	15.47686900	-0.50616000	-1.70839600
H	15.32923800	0.38504300	-3.22604300
H	15.88333700	1.21426400	-1.77441300
C	10.52502500	-0.51741600	-0.21251200
C	10.24704000	-1.87620700	-0.84470000
H	11.15370200	-2.49148400	-0.81554700
H	9.45841500	-2.42844600	-0.32520000
H	9.94828500	-1.76903200	-1.89301100
C	10.94337300	-0.62940500	1.26318400
H	11.15595400	0.36614500	1.67086800
H	10.16445700	-1.09484500	1.87618100
H	11.85362800	-1.23476300	1.34688400
C	9.37237400	0.46295100	-0.31146800
C	8.04056900	0.27946600	0.11302500
H	7.34634300	1.08257700	-0.13627000
C	7.54246800	-0.78860600	0.79495600
H	8.20775100	-1.59074500	1.11344900
C	6.18528400	-0.97558700	1.17737400
C	5.67689300	-2.03532400	1.89975000
S	4.90587000	0.14111100	0.76281000
C	4.29777500	-1.95283600	2.13321600
H	6.30846500	-2.84367500	2.25842600
C	3.71908600	-0.82857500	1.59258200
H	3.73393400	-2.68364100	2.70620000
C	2.34156300	-0.41482900	1.63279800

C	1.82160400	0.84285300	1.44700700
S	1.07039100	-1.56545500	1.94039000
C	0.41655700	0.88898800	1.54483500
H	2.44391300	1.71560500	1.26759300
C	-0.14886300	-0.32767000	1.80769300
H	-0.17888100	1.79069500	1.43780800
S	-1.85169400	-0.69352700	2.03021100
C	-2.24036500	-1.35775500	0.36080900
H	-1.93481900	-0.60950500	-0.38084200
H	-1.64436500	-2.26388400	0.19649300
C	-3.72016900	-1.65673300	0.26723200
H	-4.01304900	-2.38312700	1.03707600
H	-4.30143600	-0.74467900	0.46528400
C	-4.09575700	-2.21279900	-1.10275300
H	-3.83243000	-1.48977400	-1.88739500
H	-3.50269100	-3.11710400	-1.30027700
C	-6.55245500	-1.96424700	-1.90436200
H	-6.58150800	-1.13674400	-2.60025500
C	-5.54026200	-2.55056300	-1.18878900
N	-6.07657900	-3.56982900	-0.46673600
N	-7.34840600	-3.64096500	-0.70056600
N	-7.65313000	-2.67851100	-1.57957000
C	-9.03347200	-2.45199100	-1.96072100
H	-9.05703700	-2.17100000	-3.02146400
H	-9.54212700	-3.41720600	-1.86279100
C	-9.69627300	-1.39674700	-1.09719900
H	-9.13294500	-0.45405000	-1.17658600
H	-9.62211600	-1.70995700	-0.04579800
C	-11.14586400	-1.17108500	-1.48143400
H	-11.20832000	-0.87865300	-2.54245700
H	-11.70001200	-2.12023800	-1.40281900
C	-11.82595700	-0.11681200	-0.62780900
H	-11.76458800	-0.41009000	0.43234400
H	-11.26892100	0.83114500	-0.70387000
C	-13.27617800	0.11709000	-1.00660500
H	-13.33665500	0.40604500	-2.06864900
H	-13.83390600	-0.83028600	-0.92717100
C	-13.95465200	1.17548100	-0.15708700
H	-13.89557100	0.88638000	0.90475200
H	-13.39523400	2.12207500	-0.23524800
C	-15.40420800	1.41337100	-0.53637800
H	-15.46328600	1.69874500	-1.59951200
H	-15.96498200	0.46785400	-0.45439500
C	-16.08057300	2.47656100	0.30889600
H	-16.02212300	2.19235200	1.37207400
H	-15.51994000	3.42204400	0.22661300
C	-17.52978100	2.71553500	-0.07059200
H	-17.59059400	2.99561000	-1.13518200
H	-18.09475500	1.77296100	0.01872200
C	-18.20128300	3.78602100	0.77047400
H	-18.14138000	3.51117000	1.83373900
H	-17.64083400	4.72928300	0.67735200
C	-19.65918300	4.02216100	0.38856100
H	-19.71861400	4.30923500	-0.67165400
H	-20.23499100	3.09915000	0.55134100
C	9.17307900	2.86884200	-0.81526100
H	8.08441200	2.79222400	-0.80717800
H	9.49878700	3.48996300	-1.65202900
C	9.66340000	3.56066500	0.59771100
H	9.10409400	2.87533900	1.31256900

H	9.09905600	4.53652300	0.57116300
O	10.93571000	3.59965600	0.71602500
N	9.79454800	1.59750900	-0.88687700
H	-20.07521400	4.82837400	1.01060600

IND1 open form, conformer 3

C	10.60823400	2.77990600	-0.05179500
C	11.41519800	1.74437600	-0.49351900
C	12.75495400	1.96041500	-0.73237600
C	13.28996900	3.23505800	-0.53311200
C	12.45634200	4.25173800	-0.06532900
C	11.10925700	4.04540600	0.19124400
H	13.40284400	1.14705100	-1.06227800
H	12.88373100	5.23552300	0.12176000
H	10.49472900	4.84001100	0.59956300
C	14.73220400	3.50605800	-0.82720800
H	15.35961400	2.63301300	-0.61776900
H	14.88227600	3.76298300	-1.88385900
H	15.11575300	4.34279200	-0.23471300
C	10.61108600	0.47462400	-0.50281300
C	10.74768900	-0.28742600	-1.81348800
H	11.79933200	-0.54262300	-1.98728900
H	10.18143300	-1.22318300	-1.81884900
H	10.40524700	0.31769300	-2.65994900
C	11.06253500	-0.34785900	0.71954600
H	10.96907700	0.25973300	1.62837400
H	10.46695800	-1.25862300	0.84341700
H	12.11373900	-0.63645800	0.60163800
C	9.22059900	0.99960400	-0.20478400
C	8.00555100	0.28495800	-0.19881800
H	7.10320500	0.88128100	-0.05802200
C	7.85427600	-1.05945400	-0.35699200
H	8.73373600	-1.69717000	-0.44075100
C	6.62349700	-1.76788800	-0.39895300
C	6.46994900	-3.13526900	-0.50463400
S	5.05809200	-0.99135300	-0.33353900
C	5.13559500	-3.55967300	-0.50929200
H	7.32332600	-3.80657400	-0.55486200
C	4.23314700	-2.52372800	-0.42145400
H	4.82636500	-4.60005200	-0.54366200
C	2.79826200	-2.61248400	-0.42657100
C	2.02210400	-3.61798300	-0.93674200
S	1.79219300	-1.37433100	0.29291000
C	0.63553700	-3.41160000	-0.77276200
H	2.44379400	-4.47710500	-1.45107200
C	0.34357200	-2.23494100	-0.13508700
H	-0.11801000	-4.10422500	-1.13202900
S	-1.19591800	-1.51422300	0.29127500
C	-2.32071400	-2.87476100	-0.15543600
H	-2.24369800	-3.05755100	-1.23526200
H	-1.99936000	-3.78110500	0.37331300
C	-3.73820200	-2.50484000	0.22895300
H	-3.81050900	-2.34304500	1.31181400
H	-4.02900100	-1.55811700	-0.24790100
C	-4.71752800	-3.60171600	-0.17313100
H	-4.71764600	-3.72902200	-1.26468500
H	-4.37580100	-4.55881200	0.24868100
C	-7.27440400	-3.19904200	-0.38938700
H	-7.52120300	-3.24686200	-1.44121700
C	-6.09875600	-3.33033600	0.30418400

N	-6.37593800	-3.18268900	1.62667400
N	-7.64491600	-2.97458000	1.77978200
N	-8.20727700	-2.98977700	0.56588800
C	-9.62676100	-2.72957200	0.42325300
H	-9.99481200	-3.31204300	-0.43090200
H	-10.10549600	-3.12833300	1.32446500
C	-9.93663400	-1.25465100	0.25821100
H	-9.42736400	-0.86878900	-0.63820600
H	-9.51167500	-0.71015300	1.11346000
C	-11.42987500	-1.00742900	0.16204900
H	-11.84609000	-1.57585100	-0.68588000
H	-11.92471600	-1.41155800	1.05979200
C	-11.78982600	0.45905700	0.00988100
H	-11.36728100	1.02926100	0.85244400
H	-11.30822700	0.86564800	-0.89393200
C	-13.28684200	0.69404100	-0.06125500
H	-13.70785100	0.12337400	-0.90516800
H	-13.76370200	0.27858700	0.84135200
C	-13.66690600	2.15647400	-0.20134700
H	-13.24222600	2.72828600	0.63961700
H	-13.19932400	2.57410300	-1.10772500
C	-15.16666200	2.37883200	-0.25636000
H	-15.59044800	1.81062600	-1.10057900
H	-15.63170800	1.95242800	0.64742700
C	-15.55974400	3.83911100	-0.38232200
H	-15.13541300	4.40781600	0.46092200
H	-15.10034400	4.26816800	-1.28753000
C	-17.06108800	4.05202700	-0.42834200
H	-17.48657200	3.49005400	-1.27603600
H	-17.52117700	3.61698500	0.47409400
C	-17.45998300	5.51254800	-0.53961100
H	-17.03828000	6.07518500	0.30619100
H	-17.00560300	5.95027400	-1.44181800
C	-18.97114600	5.71760300	-0.58148500
H	-19.39021200	5.18083200	-1.44534800
H	-19.41972900	5.32882200	0.34459500
C	8.36006900	3.02352800	0.89415900
H	7.32673100	2.74237400	0.68068400
H	8.49285100	4.09666100	0.74485000
C	8.71462000	2.61599900	2.45030800
H	8.32483900	1.54707300	2.41945900
H	7.96185200	3.22127100	3.03036900
O	9.95479600	2.75951900	2.73397200
N	9.28696900	2.30510500	0.09143800
H	-19.19309800	6.79100800	-0.67389200